Frequency characterization of a swept- and fixed-wavelength external-cavity quantum cascade laser by use of a frequency comb

Kevin Knabe,[1,*] Paul A. Williams,[1] Fabrizio R. Giorgetta,[1] Chris M. Armacost,[2] Sam Crivello,[2] Michael B. Radunsky,[2] and Nathan R. Newbury[1]

[1]*National Institute of Standards and Technology, Optoelectronics Division, 325 Broadway, Boulder, Colorado 80305, USA*

[2]*Daylight Solutions, 15378 Avenue of Science, Suite 200, San Diego, California 92128, USA*

[*]*kevin.knabe@nist.gov*

Abstract: The instantaneous optical frequency of an external-cavity quantum cascade laser (QCL) is characterized by comparison to a near-infrared frequency comb. Fluctuations in the instantaneous optical frequency are analyzed to determine the frequency-noise power spectral density for the external-cavity QCL both during fixed-wavelength and swept-wavelength operation. The noise performance of a near-infrared external-cavity diode laser is measured for comparison. In addition to providing basic frequency metrology of external-cavity QCLs, this comb-calibrated swept QCL system can be applied to rapid, precise broadband spectroscopy in the mid-infrared spectral region.

OCIS codes: (300.6390) Spectroscopy, molecular; (140.4050) Mode-locked lasers; (190.4223) Nonlinear wave mixing.

References and links

1. R. F. Curl, F. Capasso, C. Gmachl, A. A. Kosterev, B. McManus, R. Lewicki, M. Pusharsky, G. Wysocki, and F. K. Tittel, "Quantum cascade lasers in chemical physics," Chem. Phys. Lett. **487**(1-3), 1–18 (2010).
2. A. Kosterev, G. Wysocki, Y. Bakhirkin, S. So, R. Lewicki, M. Fraser, F. Tittel, and R. Curl, "Application of quantum cascade lasers to trace gas analysis," Appl. Phys. B **90**(2), 165–176 (2008).
3. S. Borri, S. Bartalini, P. C. Pastor, I. Galli, G. Giusfredi, D. Mazzotti, M. Yamanishi, and P. De Natale, "Frequency-noise dynamics of mid-infrared quantum cascade lasers," IEEE J. Quantum Electron. **47**(7), 984–988 (2011).
4. M. S. Taubman, T. L. Myers, B. D. Cannon, R. M. Williams, F. Capasso, C. Gmachl, D. L. Sivco, and A. Y. Cho, "Frequency stabilization of quantum-cascade lasers by use of optical cavities," Opt. Lett. **27**(24), 2164–2166 (2002).
5. G. Wysocki, R. Lewicki, R. F. Curl, F. K. Tittel, L. Diehl, F. Capasso, M. Troccoli, G. Hofler, D. Bour, S. Corzine, R. Maulini, M. Giovannini, and J. Faist, "Widely tunable mode-hop free external cavity quantum cascade lasers for high resolution spectroscopy and chemical sensing," Appl. Phys. B **92**(3), 305–311 (2008).
6. R. Maulini, A. Mohan, M. Giovannini, J. Faist, and E. Gini, "External cavity quantum-cascade laser tunable from 8.2 to 10.4 μm using a gain element with a heterogeneous cascade," Appl. Phys. Lett. **88**(20), 201113 (2006).
7. H. L. Zhang, C. Peng, A. Seetharaman, G. P. Luo, H. Q. Le, C. Gmachl, D. L. Sivco, and A. Y. Cho, "External-cavity tunable mid-infrared laser using off-band surface-emitting bragg grating coupler," Appl. Phys. Lett. **86**(11), 111112 (2005).
8. M. Pushkarsky, M. Weida, T. Day, D. Arnone, R. Pritchett, D. Caffey, and S. Crivello, "High-power tunable external cavity quantum cascade laser in the 5-11 μm regime," Proc. SPIE **6871**, 68711X, 68711X-8 (2008).
9. A. Gambetta, D. Gatti, A. Castrillo, G. Galzerano, P. Laporta, L. Gianfrani, and M. Marangoni, "Mid-infrared quantitative spectroscopy by comb-referencing of a quantum-cascade-laser: Application to the CO(2) spectrum at 4.3 μm," Appl. Phys. Lett. **99**(25), 251107 (2011).
10. D. Gatti, A. Gambetta, A. Castrillo, G. Galzerano, P. Laporta, L. Gianfrani, and M. Marangoni, "High-precision molecular interrogation by direct referencing of a quantum-cascade-laser to a near-infrared frequency comb," Opt. Express **19**(18), 17520–17527 (2011).
11. I. Coddington, F. R. Giorgetta, E. Baumann, W. C. Swann, and N. R. Newbury, "Characterizing fast arbitrary cw waveforms with 1500 THz/s instantaneous chirps," IEEE J. Sel. Top. Quantum Electron. **18**(1), 228–238 (2012).
12. F. R. Giorgetta, I. Coddington, E. Baumann, W. C. Swann, and N. R. Newbury, "Fast high-resolution

#166274 - $15.00 USD Received 9 Apr 2012; revised 30 Apr 2012; accepted 4 May 2012; published 16 May 2012

spectroscopy of dynamic continuous-wave laser sources," Nat. Photonics **4**(12), 853–857 (2010).
13. Z. W. Barber, F. R. Giorgetta, P. A. Roos, I. Coddington, J. R. Dahl, R. R. Reibel, N. Greenfield, and N. R. Newbury, "Characterization of an actively linearized ultrabroadband chirped laser with a fiber-laser optical frequency comb," Opt. Lett. **36**(7), 1152–1154 (2011).
14. S. Bartalini, P. Cancio, G. Giusfredi, D. Mazzotti, P. De Natale, S. Borri, I. Galli, T. Leveque, and L. Gianfrani, "Frequency-comb-referenced quantum-cascade laser at 4.4 microm," Opt. Lett. **32**(8), 988–990 (2007).
15. A. Castrillo, E. De Tommasi, L. Gianfrani, L. Sirigu, and J. Faist, "Doppler-free saturated-absorption spectroscopy of CO2 at 4.3 microm by means of a distributed feedback quantum cascade laser," Opt. Lett. **31**(20), 3040–3042 (2006).
16. L. S. Rothman, I. E. Gordon, A. Barbe, D. C. Benner, P. E. Bernath, M. Birk, V. Boudon, L. R. Brown, A. Campargue, J. P. Champion, K. Chance, L. H. Coudert, V. Dana, V. M. Devi, S. Fally, J. M. Flaud, R. R. Gamache, A. Goldman, D. Jacquemart, I. Kleiner, N. Lacome, W. J. Lafferty, J. Y. Mandin, S. T. Massie, S. N. Mikhailenko, C. E. Miller, N. Moazzen-Ahmadi, O. V. Naumenko, A. V. Nikitin, J. Orphal, V. I. Perevalov, A. Perrin, A. Predoi-Cross, C. P. Rinsland, M. Rotger, M. Simeckova, M. A. H. Smith, K. Sung, S. A. Tashkun, J. Tennyson, R. A. Toth, A. C. Vandaele, and J. Vander Auwera, "The HITRAN 2008 molecular spectroscopic database," J. Quant. Spectrosc. Radiat. Transf. **110**(9-10), 533–572 (2009).
17. L. Tombez, J. Di Francesco, S. Schilt, G. Di Domenico, J. Faist, P. Thomann, and D. Hofstetter, "Frequency noise of free-running 4.6 μm distributed feedback quantum cascade lasers near room temperature," Opt. Lett. **36**(16), 3109–3111 (2011).
18. S. Bartalini, S. Borri, I. Galli, G. Giusfredi, D. Mazzotti, T. Edamura, N. Akikusa, M. Yamanishi, and P. De Natale, "Measuring frequency noise and intrinsic linewidth of a room-temperature DFB quantum cascade laser," Opt. Express **19**(19), 17996–18003 (2011).
19. S. Bartalini, S. Borri, P. Cancio, A. Castrillo, I. Galli, G. Giusfredi, D. Mazzotti, L. Gianfrani, and P. De Natale, "Observing the intrinsic linewidth of a quantum-cascade laser: Beyond the schawlow-townes limit," Phys. Rev. Lett. **104**(8), 083904 (2010).

1. Introduction

Quantum cascade lasers (QCLs) have developed rapidly in past years and have opened up new possibilities in spectroscopic sensing in the mid-infrared (mid-IR) [1,2]. As with any laser used for spectroscopy, an important property of QCL systems is the laser linewidth, or more accurately, the frequency noise power spectral density of the laser. The frequency noise power spectral density of a QCL can provide important information about the fundamental behavior of the QCL [3]. While there has been significant research on the frequency noise of distributed feedback (DFB) QCLs by use of both gas absorption lines and frequency combs [3,4], the frequency noise of tunable external-cavity QCLs has not been analyzed as completely. In this paper, we present measurements of the frequency noise of a commercial external-cavity QCL while the wavelength is swept at close to a terahertz per second. Furthermore, we show that the combination of a frequency comb and external-cavity QCL will allow for precise broadband spectroscopy over terahertz tuning bandwidths in the mid-IR.

External-cavity QCLs, as with their cousins, external-cavity diode lasers, can provide much broader spectral tuning than DFB-based devices can. In recent years, external-cavity QCLs have seen significant improvements in output power, linewidth, and mode-hop-free optical-frequency tuning range [5–8]. These lasers have obvious applications to broadband optical sensing because they can be swept over an entire rovibrational band of one or more molecules. However, to use external-cavity QCLs for precision spectroscopy with broad spectral coverage, it is critical to quantify the frequency noise during the two typical operational modes of fixed-wavelength or swept-wavelength operation. In fixed wavelength operation, the grating position of the external-cavity QCL is fixed and therefore its wavelength is nominally fixed. However, the true wavelength, or optical frequency, of the external cavity QCL will still vary as it is not locked to an absolute reference. In swept-wavelength operation the grating position of the external-cavity QCL is changed in order to sweep the QCL wavelength over a broad bandwidth rapidly. With appropriate design, this sweep can be mode-hop free, but there will invariably be significant instantaneous frequency deviations from the expected sweep that are large in comparison to the intrinsic laser linewidth. In both the fixed and swept-wavelength modes, we are interested in quantifying the

#166274 - $15.00 USD Received 9 Apr 2012; revised 30 Apr 2012; accepted 4 May 2012; published 16 May 2012

frequency noise on the external-cavity QCL to determine its deviation from the ideal behavior (of a truly fixed wavelength output or a truly linear wavelength sweep).

Here we have measured the frequency-noise power spectral density of a commercial external-cavity QCL operating at 4.5 μm through comparison with a near-IR fiber frequency comb. Our approach combines the detection method pioneered by Gatti et al. [9,10], with the acquisition and analysis method of Refs [11–13]. With this setup, we are able to continuously track the frequency output of the external-cavity QCL at a time resolution as short as 20 ns and kilohertz-level frequency resolution. This approach allows us to measure the instantaneous optical frequency of the external-cavity QCL when operated both at a fixed wavelength and during swept operation. An analysis of deviations of the instantaneous optical frequency from a fixed value (for the fixed-wavelength operation) or from a linear fit (for the swept operation) yields the frequency-noise power spectral density. We find that the frequency-noise power spectral density for fixed-wavelength operation is commensurate with that measured for DFB-QCLs. This noise remains unchanged for a small tuning range implemented with a piezoelectric transducer (PZT). For larger (terahertz) tuning ranges, the motion of the grating in the external-cavity QCL leads to an overall increase in the frequency noise at low frequency offsets. This increase is very similar to that observed for near-IR external-cavity diode lasers.

In addition to the basic metrology of the external-cavity QCL, this system allows for high-precision spectroscopy. Similar comb-assisted spectroscopy has been demonstrated with DFB QCLs by effectively locking the DFB QCL to the comb [9,14]. Here instead, we simultaneously record the instantaneous frequency of the external-cavity QCL and the gas absorption. High-accuracy spectra can be acquired rapidly (within the 1 second sweep time of the laser) and over a broad bandwidth without the need to feedback to actively stabilize the external-cavity QCL. As an example, we show a corrected absorption profile of an N_2O absorption line. While this approach cannot yield line centers to the same accuracy of a QCL locked to a saturated absorption line (as in Ref [15].) it should easily reach sub-megahertz accuracies while allowing greater frequency agility. Moreover, the measurement of the entire absorption line should allow for accurate measurements of lineshape and a correspondingly accurate measurement of the gas concentration. Essentially, the system can combine the sensitivity expected from the QCL swept laser with the accuracy of the frequency comb.

2. Experimental method

The heart of this technique combines the optical setup of Ref [10]. and the frequency-tracking technique of Refs [12,13], and is shown schematically in Fig. 1(a). A near-IR fiber frequency comb centered at 1550 nm is combined with a mid-IR external-cavity QCL at 4500 nm in a nonlinear crystal to produce a new frequency comb in the near-IR centered at 1150 nm via sum-frequency generation (called here the “QCL comb”). The QCL comb contains the frequency characteristics of the external-cavity QCL laser added with the near-IR frequency comb. The frequency behavior of the external-cavity QCL can then be measured by heterodyning the QCL comb with a supercontinuum comb (SC) generated from the spectrally-broadened near-IR comb.

#166274 - $15.00 USD Received 9 Apr 2012; revised 30 Apr 2012; accepted 4 May 2012; published 16 May 2012

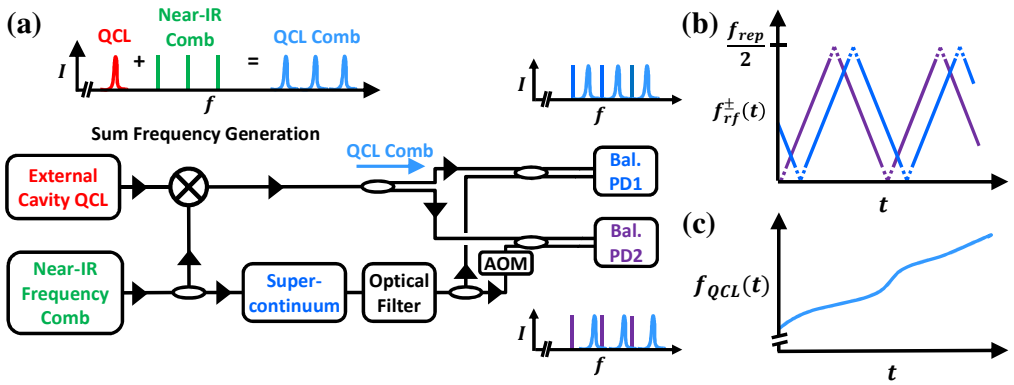

Fig. 1. (a) Schematic of the system to measure the instantaneous frequency of the external-cavity QCL with a near-IR frequency comb. The output of the QCL (red Lorentzian) is summed with the output of a near-IR fiber frequency comb (green) to generate a QCL comb (light blue Lorentzians), as illustrated schematically in the top graph. This QCL comb is then combined with a supercontinuum comb, generated by spectrally broadening the original near-IR frequency comb, and detected with two balanced photodiodes (PD1 and PD2). The QCL and SC combs (blue and purple) overlap spectrally, as illustrated near the PDs, and their instantaneous heterodyne frequency is a measure of the instantaneous QCL frequency. The supercontinuum comb directed onto PD2 has been shifted in frequency by an acousto-optic modulator (AOM) to circumvent Nyquist ambiguities. Ovals indicate optical couplers. (b) The heterodyne rf frequencies measured at each photodetector (PD1 in blue, PD2 in purple) versus time for a swept QCL. Near the Nyquist frequency, $f_{rep}/2$, and DC, the rf frequencies are ill-defined and shown as dotted lines. (c) The two rf-heterodyne frequencies of (b) can be unwrapped to yield the instantaneous QCL frequency, $f_{QCL}(t)$, versus time during a sweep.

The detected heterodyne signal between the QCL and SC combs is low-pass filtered at $f_{rep}/2$ (the Nyquist frequency) and digitized at the comb repetition frequency f_{rep}. The digitized signal from the photodetector (PD1) exhibits two instantaneous rf frequencies given by $f_{rf}^{+}(t) = f_{QCL}(t) - p \cdot f_{rep}$ and $f_{rf}^{-}(t) = -f_{QCL}(t) + (p+1) \cdot f_{rep}$, where $f_{QCL}(t)$ is the instantaneous optical frequency of the QCL. The integer p equals $f_{QCL}(t)/f_{rep}$ rounded down to the nearest integer so that both $f_{rf}^{+}(t)$ and $f_{rf}^{-}(t)$ are positive and less than f_{rep} [9]. As the QCL frequency is swept, the observed rf signal frequency alternates between the frequencies $f_{rf}^{+}(t)$ and $f_{rf}^{-}(t)$ as only one of these two heterodyne signals will lie below the rf Nyquist frequency at a given point in time. This results in the triangular rf frequencies shown in Fig. 1(b). Since the instantaneous rf frequency is ill-defined at $f_{rep}/2$ (i.e., when the QCL comb bisects the SC comb) and DC (when these combs directly overlap), a second detection path is added with the SC comb frequency shifted by $f_{rep}/4$ [12] to generate a quadrature-shifted triangular waveform. If the QCL optical frequency sweep is continuous (i.e. mode-hop free), then these measured rf frequencies can be unwrapped to yield the relative instantaneous QCL optical frequency [11,13].

In the actual analysis, we monitor the data for mode-hops, evident in either the QCL intensity or unwrapped frequency versus time. The instantaneous rf frequency is calculated based on the derivative of the instantaneous phase, which in turn is calculated using a Hilbert transform of the digitized rf signal. If a central-difference is used to estimate the derivative of the phase, the effective time resolution is 20 ns [11–13]. However, in cases where the signal-to-noise ratio is low, the phase estimation can include 2π slips that lead to "glitches" in the retrieved instantaneous frequency. To avoid these glitches, a bandpass filter whose center

#166274 - $15.00 USD Received 9 Apr 2012; revised 30 Apr 2012; accepted 4 May 2012; published 16 May 2012

tracks the peak of the rf heterodyne signal is applied in post-processing with an effective bandwidth of 5 MHz. This effectively reduces the time resolution of the system to 200 ns.

Transferring the external-cavity QCL frequency characteristics into the near-IR has several benefits, as noted in Ref [10]. and reiterated here. First, the optical signal used to characterize the QCL lies in the near-IR, where single-mode fiber, telecomm components, and low-noise photodetectors are readily available. Second, for QCL wavelengths ranging from 3.50 μm to 10.0 μm, the up-converted QCL comb wavelength falls in the range of 1.08 μm to 1.35 μm, well within the spectral coverage of a supercontinuum fiber comb. Finally, as with other comb-based QCL techniques, the carrier-envelope offset frequency $\left(f_{CEO}\right)$ is directly cancelled as common-mode fluctuations. Therefore there are no requirements for f_{CEO} stabilization, and the measured QCL frequency is absolute (provided the integer p is known). The value of p can be found by measurement of a gas reference cell in combination with a molecular database with accuracy better than f_{rep} (such as HITRAN [16]), or by the addition of a second frequency comb with a different repetition rate [12]. In principle, this technique enables realization of absolute frequency accuracies limited only by the comb's repetition rate accuracy. An accuracy of 10 millihertz in 1 second on the 100 MHz repetition rate, which is easily achieved for frequency combs, corresponds to a 10^{-10} fractional frequency accuracy, or 7 kHz accuracy at 4500 nm, which is well below current molecular line accuracies in the mid-IR [16]. The results in this work do not include calculation of the integer p by the aforementioned methods, and the relative QCL optical frequency excludes an exact offset of $p \cdot f_{rep}$ (where p is calculated at time $t = 0$).

3. Experimental setup

We measure a Daylight Solutions tunable mid-IR external-cavity QCL system operating around 4500 nm, at room temperature, with a maximum output power of 300 mW by use of the setup shown in Fig. 2. The erbium-doped, femtosecond fiber ring laser operates at ~100 MHz repetition rate with a center wavelength of 1565 nm, and has a full-width-at-half-maximum optical bandwidth of 30 nm. The fiber-laser output is split into two arms by use of an AOM as a 50/50 splitter, and is amplified in each arm to about 100 mW. One arm supplies the near-IR comb and is overlapped with the external-cavity QCL light inside a 2.4 mm long periodically poled lithium niobate (PPLN) crystal with a poling period of 28.2 μm. Optimal phase matching occurs for this PPLN in a 44 nm (5.6 THz) FWHM bandwidth around 1539 nm, corresponding to 4 mW of near-IR comb power. Sum-frequency generation with 100 mW of the QCL beam yields an up-converted QCL comb at 1147 nm with a bandwidth of 22 nm (5.0 THz) and a power of 140 nW (see Fig. 2). The nonlinear conversion efficiency is 4×10^{-4} W^{-1}, in agreement with theoretical simulations. The cw QCL light is removed via a silica wedge, and the QCL comb light is then coupled into single-mode fiber (7 dB insertion loss). The residual near-IR comb is removed by use of a 1300/1550 nm wavelength division multiplexer (WDM) and a 44 cm piece of unpumped, highly-doped erbium fiber.

The second amplified copy of the fiber laser output is broadened in 17.5 cm of highly nonlinear fiber (HNLF) to form a supercontinuum comb and filtered to 20 nm at the QCL comb center wavelength for spectral overlap. The supercontinuum is then combined with the QCL comb and the resulting heterodyne signal is detected on a 100 MHz balanced PD. Because both combs' outputs are pulses in the time domain, optical delay lines are used to ensure temporal overlap at the photodiode. To address the Nyquist ambiguity mentioned in the previous section, a second branch generates a SC comb shifted by $f_{rep}/4$, which also mixes with the QCL comb to generate a heterodyne signal on a second balanced photodiode. The outputs from both balanced detectors are digitized synchronously with the comb

#166274 - $15.00 USD Received 9 Apr 2012; revised 30 Apr 2012; accepted 4 May 2012; published 16 May 2012

repetition rate and processed as discussed in Section 2 to yield the instantaneous QCL frequency.

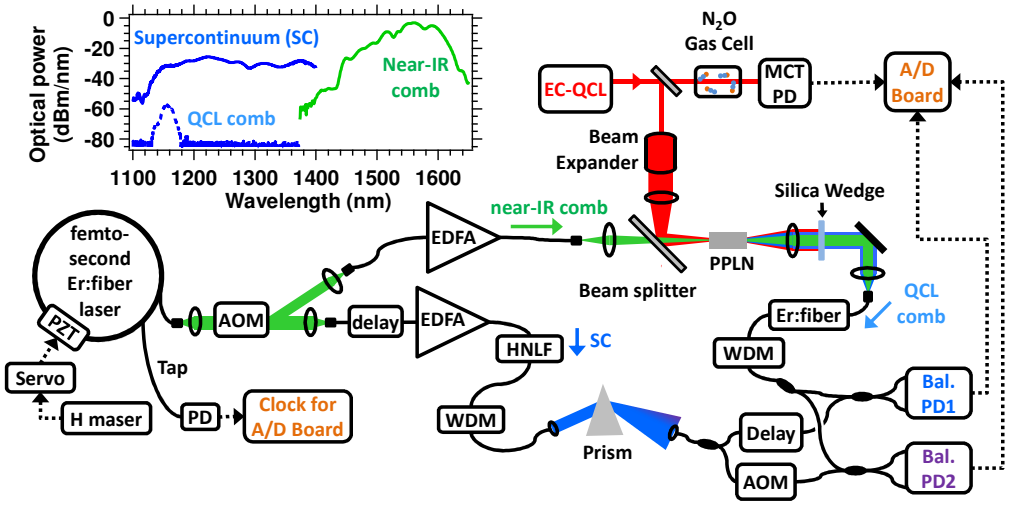

Fig. 2. Experimental realization of Fig. 1. It should be noted that most of the setup is contained within fiber and could be adapted to a portable setup. Solid lines indicate optical fiber; the thick colored lines are indicative of free space beams and their relative size; and dashed line indicates an electrical cable. Optical spectra of the near-IR comb, SC, and QCL comb are provided in the upper left graph. Erbium-doped fiber amplifier (EDFA) and HgCdTe photodetector (MCT PD).

4. Noise characterization of a fixed-wavelength external-cavity QCL

We first discuss the frequency noise of the external-cavity QCL at a fixed wavelength (where by "fixed" we mean that the grating position in the cavity is fixed but no active feedback control signals are sent to stabilize the QCL's optical frequency). In this case, as long as the QCL's optical frequency remains within a 50 MHz span, the signal is simply the beat note of the up-converted QCL comb teeth with the adjacent SC comb teeth. The processing yields the instantaneous frequency versus time with 200 ns time resolution. These data can then be analyzed at different time-bandwidth limited resolutions. Figure 3(a) presents these data as a spectrogram (or short-time Fourier transform) where we have selected a time resolution of 33 μs, and therefore a frequency resolution of 30 kHz. These same data can also be used to generate the power spectrum, or lineshape, of the QCL laser for different observation times, as shown in Fig. 3(b). The FWHM external-cavity QCL linewidth is measured to be 15 MHz, 4 MHz, and 1 MHz in 50 ms, 1.3 ms, and 10 μs windows, respectively.

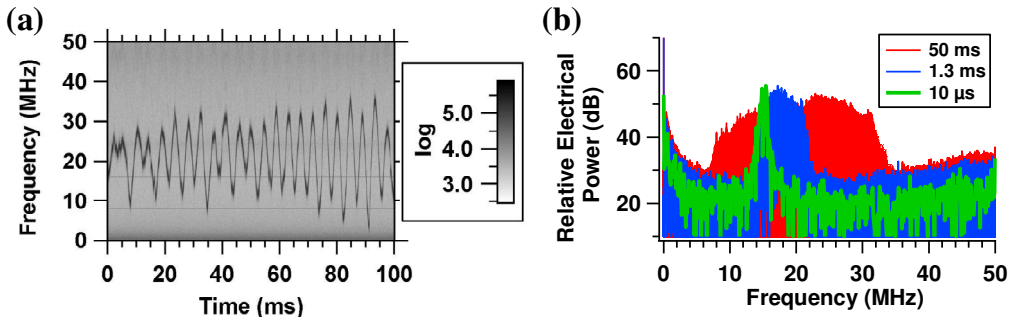

Fig. 3. (a) Spectrogram (short-period Fourier transform) of the free-running external-cavity QCL optical frequency versus time. The amplitude of the power spectrum is given (arbitrary units) by shades of gray detailed in the legend. The dark black trace centered around 20 MHz

#166274 - $15.00 USD Received 9 Apr 2012; revised 30 Apr 2012; accepted 4 May 2012; published 16 May 2012

represents the instantaneous frequency of the external-cavity QCL. The frequency resolution is 30 kHz and the time resolution is 33 μs. The additional horizontal lines at 8 MHz and 16 MHz are experimental artifacts. (b) Power spectra for different time windows.

The frequency-noise power spectral density (PSD) from 20 Hz to 2 MHz of the external-cavity QCL is shown in Fig. 4. We compare this measurement to the noise of room-temperature DFB QCLs (blue shaded region) [17,18], and find the external-cavity QCL to have a higher noise level. The external-cavity QCL frequency noise falls off as $1/f^2$ at low frequencies and $1/f$ at high frequencies. In contrast, DFB QCLs have frequency noise that falls off as $1/f$ at close-in frequencies and as $1/f^2$ at higher frequencies [17,18]. This $1/f$ noise may be due to intrinsic current noise in the DFB devices. One would expect the longer cavity length of the external-cavity QCL to suppress this intrinsic noise at the cost of additional acoustic noise, and the close-in $1/f^2$ data of Fig. 4 is consistent with this picture. We suspect that current driver noise is responsible for the $1/f$ behavior farther out. The Allan deviation of the QCL's frequency was calculated for short periods, and remains below 10 MHz over the full measurement range (see inset of Fig. 4).

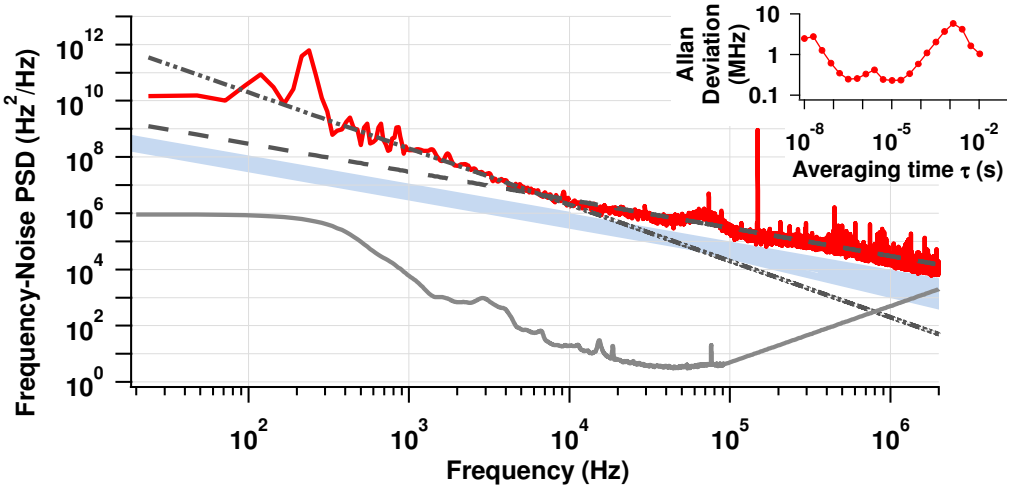

Fig. 4. Frequency-noise power spectral density for fixed-wavelength operation (red trace). The shaded light-blue region shows the range of published frequency-noise values of room-temperature DFB QCLs [17,18]. Also shown are the noise floor (gray line) and dashed asymptotes of value $\left(2\times10^{14}\right)/f^2$ and $\left(3\times10^{10}\right)/f$. The discrete spectral components above 100 kHz are likely due to noise on the current driver. Inset: The Allan deviation of the external-cavity QCL frequency versus averaging period τ.

The system noise floor (gray curve of Fig. 4) has two contributions included: the residual noise on the repetition rate of the frequency comb, and the detection noise floor. The latter gives rise to white phase noise, which translates to a frequency-noise floor that increases as f^2 [11]. The resulting noise floor is very low at acoustic frequencies due to residual repetition-rate noise on the frequency comb, but the increase at higher Fourier frequencies masks the fundamental QCL white frequency noise floor (which would yield the fundamental QCL linewidth [17,19]). A measurement of the QCL white frequency noise floor would be extremely challenging with this approach as it would require a significant increase in the QCL comb power (by increasing the near-IR comb power, the QCL power, and/or a longer piece of PPLN) and decrease in the technical QCL noise. To determine the system noise floor, we measured the comb noise at 1550 nm by comparison with a cw laser stabilized to an optical

#166274 - $15.00 USD Received 9 Apr 2012; revised 30 Apr 2012; accepted 4 May 2012; published 16 May 2012

cavity. The noise level measured in this way is a worst-case noise level, since it includes noise from f_{CEO}. Its contribution to the noise floor at the QCL frequency of ~66 THz is found by multiplying the near-IR comb noise at 1550 nm by a factor of $\left(66\,\mathrm{THz}/192\,\mathrm{THz}\right)^2$.

5. Noise characterization of a swept-wavelength external-cavity QCL

The noise characteristics of the external-cavity QCL while its optical frequency is rapidly swept are of interest for general laser characterization and precision spectroscopy. For these data, we fit the measured QCL optical frequency to $f_{QCL}(t) = f_{QCL}(0) + C \cdot t$. The fit parameters are the initial optical frequency, $f_{QCL}(0)$, and the average sweep rate, C. The residuals from this fit, $\delta f_{QCL}(t)$, are the frequency noise (or deviations from a linear sweep) of the laser. Sinusoidal modulations were also applied to change the optical frequency, and in these cases the linear term is replaced by a sine function.

Figure 5 shows the results for a linear sweep at the highest possible sweep rate of almost 1 THz/s (red curve, lower axis). The linear fit (blue dashed line, lower axis) yields the average sweep rate, and the residuals (blue trace, upper axis) are on the order of 10 GHz (or 1% of the swept bandwidth).

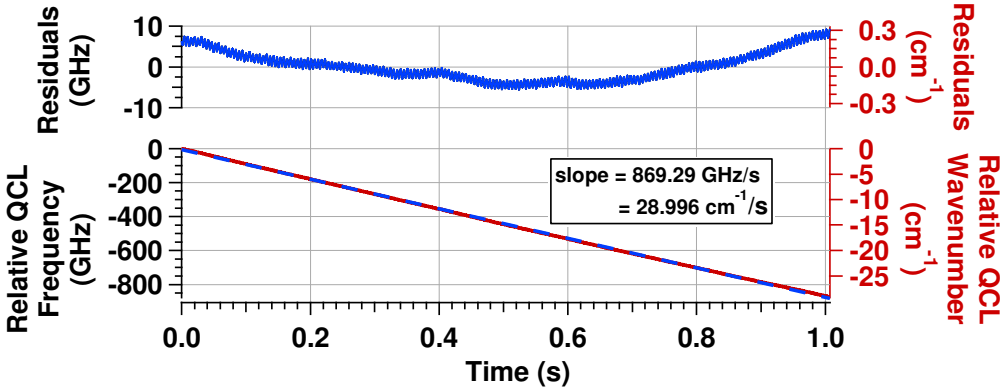

Fig. 5. Measured relative QCL frequency versus time (red line, lower axes), linear fit (dashed blue line, lower axes), and residuals from the fit (blue line, top axes) for 1 s. The average linear sweep rate is 869.29 GHz/s.

Similar data were taken for different sweeps by use of either the PZT for smaller tuning ranges or the translational stage motor on the optical grating for larger tuning ranges (as in Fig. 5). The residuals, $\delta f_{QCL}(t)$, from a series of applied sweeps were analyzed to determine the frequency-noise power spectral density and are shown in Fig. 6(a). First, we show a sinusoidal wavelength sweep that uses the PZT to modulate the grating position at 2 Hz. The maximum linear sweep rate for this modulation was 37 GHz/s. We observe very little increase in the frequency-noise power spectral density over the fixed-wavelength case, except at low acoustic frequencies (< 500 Hz). To reach broader bandwidths, the grating angle is swept by use of the translational stage motor. The frequency noise at the highest sweep rate of 870 GHz/s is shown in Fig. 6 as well (based on the residuals of Fig. 5). The frequency noise increases at frequencies below 50 kHz. One would expect an increase in any system where mechanical motion of components is necessary to achieve wavelength tuning. Frequency noise was also measured at a sweep speed of 150 GHz/s. The ratio between the noise of each of these faster sweep speeds and the noise during fixed-wavelength operation is plotted in Fig. 6(b). It is interesting to note that in certain spectral regions the noise is proportional to the sweep speed (near the 200 Hz mechanical resonance), and in other regions it is constant

#166274 - $15.00 USD Received 9 Apr 2012; revised 30 Apr 2012; accepted 4 May 2012; published 16 May 2012

(from 500 Hz to 2 kHz). It also appears that the cutoff frequency (where there is no longer an increase in noise due to sweep speed) is linear with the sweep speed.

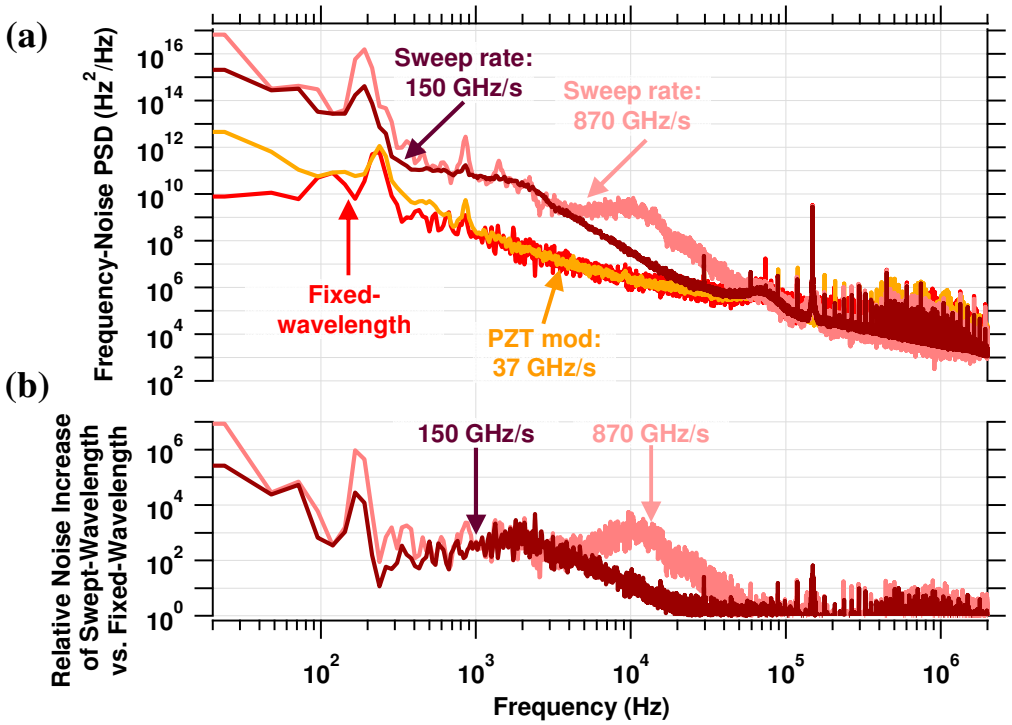

Fig. 6. (a) Frequency-noise power spectral density for a swept-wavelength external-cavity QCL with a sinusoidal PZT modulation (orange), with a high-speed linear sweep (pink), and with a medium-speed linear sweep (dark red). Also shown for comparison is the fixed-wavelength noise of Fig. 4 (light red). (b) Relative increase in noise for swept-wavelength operation versus fixed-wavelength operation.

We expect the increase in the frequency noise during a sweep to be related to the mechanical structure of any external-cavity configuration, and not specifically to the QCL. We were unable to find data in the literature on the frequency noise during a sweep of a near-IR external-cavity diode laser (ECDL). Therefore, we replaced the QCL comb in our setup with a commercial ECDL (at 1560 nm) and conducted an identical measurement. Figure 7 shows the frequency-noise PSD of the sweeping ECDL, and the relative increase in the overall frequency-noise PSD. The results are very similar to the external-cavity QCL, and confirm that sweeping external-cavity systems are susceptible to acoustic noise increases.

#166274 - $15.00 USD Received 9 Apr 2012; revised 30 Apr 2012; accepted 4 May 2012; published 16 May 2012

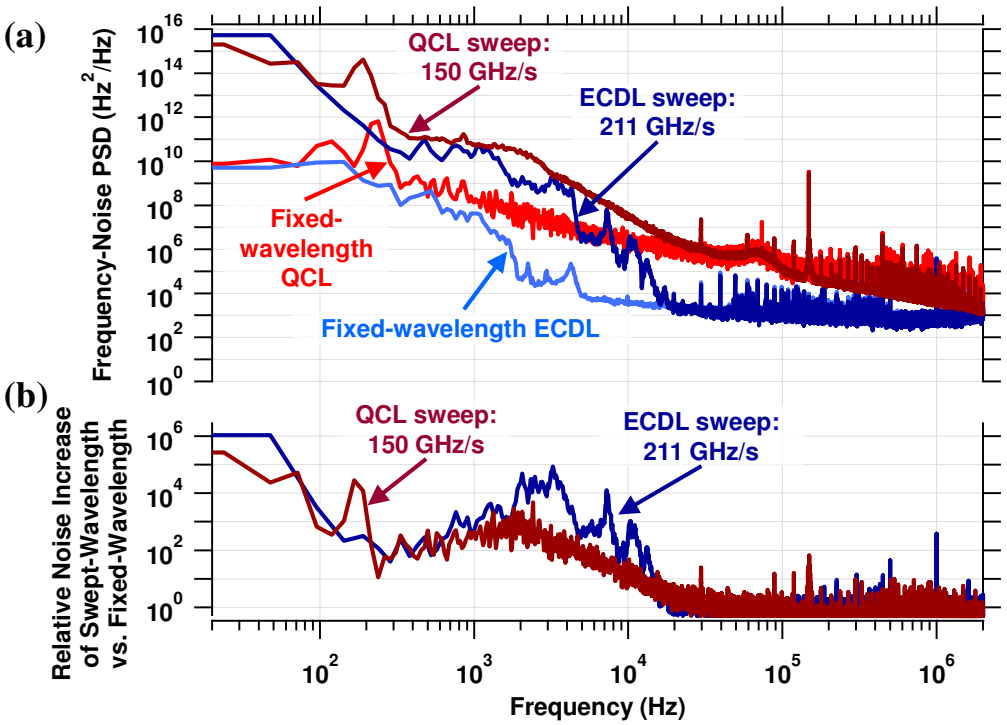

Fig. 7. (a) Frequency-noise power spectral density comparison between the external-cavity QCL and a commercial external-cavity diode laser (ECDL) for both swept- and fixed-wavelength operation. (b) Relative noise increase for swept-wavelength operation (with similar sweep-speeds) is almost identical for the external-cavity QCL and the ECDL.

6. Frequency calibration of a swept-wavelength external-cavity QCL for spectroscopy

One of the major motivations for frequency metrology of the swept external cavity QCL is to support accurate swept-laser spectroscopy with these laser systems. Nonlinearities during a laser's wavelength-sweep are a well-known issue for high-precision gas spectroscopy. The problem is illustrated in the blue data trace of Fig. 8(a), which shows the measured transmission through the N_2O gas cell of Fig. 2. The gas cell transmission is plotted versus "calculated frequency", in this case taken from the product of the nominal linear frequency sweep rate multiplied by time (and relative to the start of the sweep). The linear frequency sweep rate here was the measured, average value across the full 1 second sweep (as given for example in the legend in Fig. 5). The transmission spectrum would seem to indicate unexpected asymmetric structure in the lineshape. However, when the absorption trace is instead plotted versus the calibrated instantaneous frequency (Fig. 8(b)), the true lineshape is shown, which is symmetric and follows the expected Doppler-broadened Gaussian lineshape for these gas pressures. As these data were acquired at a sweep speed of 870 GHz/s, the entire scan of the line in Fig. 8(b) was taken in 1 ms. These data are representative of the level of distortion at this sweep speed, although particular lines can have greater or lesser distortion depending on the exact behavior of the laser as it sweeps across the line. The corresponding laser frequency noise is given in Fig. 6, which also corresponds to the ~1 GHz fast ripple evident in the residuals of Fig. 5. As shown in Fig. 6, for a slower scan, the noise can be reduced by 20 dB or more, corresponding to 10 times lower frequency excursions. At these lower levels, the distortions are reduced but still noticeable over relatively narrow Doppler-broadened lines.

#166274 - $15.00 USD Received 9 Apr 2012; revised 30 Apr 2012; accepted 4 May 2012; published 16 May 2012

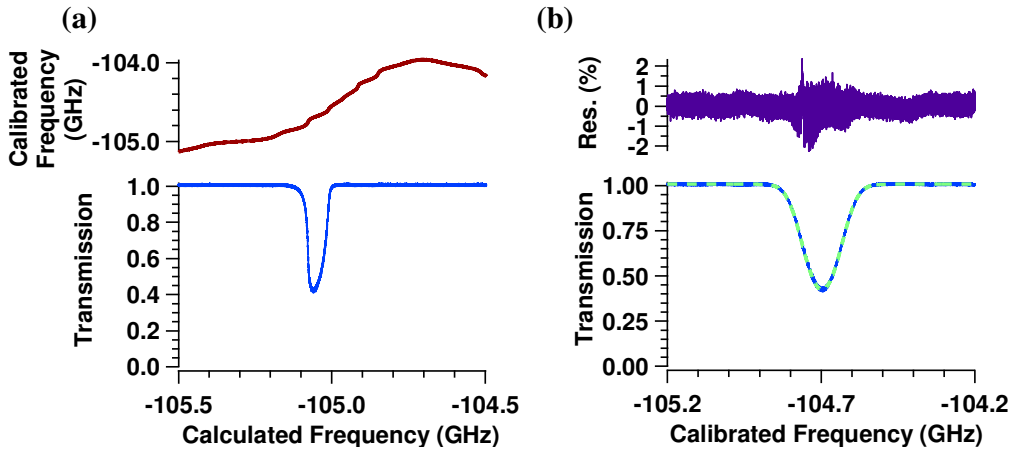

Fig. 8. (a) Top graph: True instantaneous QCL frequency versus the nominal QCL frequency calculated using the average sweep rate. Bottom graph: Transmitted intensity of the external-cavity QCL through a 4.4 Pa (33 mtorr) N_2O gas cell versus the calculated QCL frequency. (b) Rescaled transmission versus the true instantaneous QCL frequency, along with a fit assuming a Gaussian absorption line (green dashed trace) and residuals (or "Res.", purple trace). The absorption feature in (a) appears to be half as wide as the true linewidth, due to the local chirp being a factor of 2 larger than the average linear chirp. Also, the asymmetric distorted line structure from (a) is replaced with its true symmetric Gaussian shape.

7. Conclusion

We characterize the optical frequency from an external-cavity QCL for the first time to our knowledge. The optical frequency of the external-cavity QCL is measured for several conditions including a fixed-wavelength and swept-wavelength operation. The frequency noise of the external-cavity QCL is similar to DFB QCLs at 4.5 μm [17,18], but in this case is likely due to acoustical noise of the external-cavity structure. Similar noise is observed for a near-IR external-cavity diode laser when operated in a similar fashion. Finally, we show preliminary spectroscopy results in which we track the frequency output of a swept external-cavity QCL versus time while monitoring an N_2O absorption cell.

Acknowledgments

We thank Esther Baumann, Alex Zolot, Ian Coddington, Bill Swann, Lora Nugent-Glandorf, Tyler Neely, Florian Adler, and Scott Diddams for helpful discussions and the use of experimental equipment. Trade names are used only in the paper are for clarity and do not represent endorsement by NIST.

#166274 - $15.00 USD Received 9 Apr 2012; revised 30 Apr 2012; accepted 4 May 2012; published 16 May 2012